

Supporting Information (SI).

Data Collection and Generation. Gene expression data from the ECLIPSE study was collected from 220 patients classified as smoker controls (84) or COPD (136). Blood samples from each individual were profiled on Affymetrix HGU 133 plus2 microarrays. CEL data files from these assays were RMA-normalized[33] in R using the BioConductor package 'affy'[34]. Array probes were collapsed to 18895 Entrez-gene IDs using a custom CDF[35]. Finally, 1553 genes which were not matched with our motif scan (see below) were filtered out, yielding a final count of 17342 genes for which we had gene expression measurements.

Regulatory priors were created by using position weight matrices for 205 transcription factor motifs obtained from JASPAR 2014 <http://jaspar2014.genereg.net/>, [36] and running Haystack[37] to scan the hg19 genome for occurrences of these motifs. Sequences were identified as hits for a transcription factor if they satisfied the significance threshold of $p < 10^{-5}$. We then linked motifs to genes under the guidelines that a motif is a possible transcription factor binding site for a particular gene if that motif is located within 750 base pairs downstream or within 250 base pairs upstream of a gene's promoter. We applied HOMER (<http://homer.salk.edu/homer/ngs/index.html>) [38] to identify motifs that met this criteria.

Next, for each study, we identified transcription factors for which we had gene expression data, removing those regulatory edges that lacked corresponding expression values. Consequently, our motif prior consisted of 164, 164, 148, and 145 transcription factors in ECLIPSE, COPDGene, LGRC, and LTCDNM, respectively. MONSTER was run separately on each of these studies. Comparisons of differential transcription factor involvement across studies were performed on the 143 transcription factors which were common to all four studies (Figure 3).

Common network inference methods do not produce reproducible results in COPD. We evaluated the standard tools for COPD case-control studies at the network level by observing the agreement in differential network inference (NI) across studies. We utilized the four studies - ECLIPSE, COPDGene, LGRC, and LTCDNM. Our goal was to determine the ability of commonly used NI methods to find reproducible results across studies. We tested the methods Algorithm for the Reconstruction of Gene Regulatory Networks (ARACNE), Context Likelihood of Relatedness (CLR), and Weighted Gene Correlation Network Analysis (WGCNA). We computed differential edge-weights across cases and controls using each of the NI methods. Next, we plotted the differential edge-weights for each pairwise combination of studies 1. We found no meaningful correlation for edge-weight differences between *any* two studies using *any* of the three methods.

We conclude that identifying differences in COPD case-control studies using existing methods for NI do not generate reproducible results.

Inferring Gene Regulatory Networks. In 2013, we described PANDA [8], a method for estimating gene regulatory networks that uses "message passing" [40] to integrate multiple types of genomic data. PANDA begins with a prior regulatory network based on mapping transcription factor motifs to a reference

genome and integrates other sources of data, such as protein-protein interaction and gene expression profiles, to estimate individual sample networks. While PANDA has proven to be very useful in a number of applications [2, 3, 41], its iterative approach to edge-weight optimization limits its utility in situations requiring a large number of network bootstrap estimations. To address this limitation, we developed an approach which considers the available evidence of an edge for each possible TF-gene pair. This evidence can be divided into two components, referred to here as direct and indirect. Consider the edge between a TF and a gene, referred to here as TF_i and g_j , respectively. The direct evidence, $d_{i,j}$, consists of the squared conditional correlation of the g_i and g_j given all other regulators of g_i . Where g_i is the gene which encodes TF_i and \mathbf{TF} is the set of all TF genes,

$$d_{i,j} = \text{cor}(g_i, g_j | \{g_{k,-j} : k \neq j, k \in \mathbf{TF}\})^2$$

In other words, we consider the coexpression of genes for transcription factors with all other genes, conditional on the expression of the genes for other transcription factors. Naturally, the use of direct evidence alone inadequately captures regulatory relationships due to the impacts of technical noise and numerous biological external factors such as stable or transient protein-protein interactions, post-translational modifications, etc. which may confound or modify a regulatory effect. These sources of confounding and variability in the expression pattern of a gene coding a TF may obscure the effects it has on all of its target genes. Therefore it is of value if we can complement our estimate of the likelihood of a regulatory mechanism by aggregating the information from the gene expression patterns of all suspected targets of transcription factors. PANDA achieves its superior performance in part by convergence towards "agreement", whereby large collections of gene expression patterns must agree with the proposed regulatory structure in order to claim an interaction. Similarly, we look for agreement between the gene expression patterns of large sets of co-targeted genes. We refer to this feature as indirect evidence and can achieve this by again utilizing our set of regulatory priors. In this portion of the analysis we suspend the recognition of a TF as a member of the gene list and instead consider each of the m TFs to be binary classifications across the entire gene list. Class labels are determined by the presence or absence of a sequence binding motif for that TF in the vicinity of the gene.

The indirect evidence between the two nodes, $\theta_{i,j}$, represents the fitted probability that g_i belongs to the class of genes targeted by TF_j . g_i is considered to be a new observation placed into the n -dimensional space separated by transcription factor targets and non-targets. To divide up the space, we use a logistic regression on the gene expression data with outcome taken to be the existence or non-existence of a known sequence motif for TF_j in the vicinity of g_i .

$$\text{logit}(E[M_j]) = \beta_0 + \beta_1 g_{(1)} + \cdots + \beta_N g_{(n)}$$

where the response M_j is a binary vector of length n indicating the presence of a sequence motif for transcription factor j in the vicinity of each of the n genes. And where $g_{(k)}$ is a vector of length n specifying the gene expression for sample k over n genes.

For some TF-gene pair, the fitted values for each $TF_j - g_i$ pair define the “indirect” evidence $\theta_{j,i}$.

$$\hat{\theta}_{j,i} = \frac{1}{1 + e^{\beta_0 + \beta_1 g_{i,(1)} + \dots + \beta_k g_{i,(k)}}}$$

By scoring each gene according to the strength of indirect evidence for a regulatory response to each of the TFs, we can combine this with the direct evidence of regulation (squared conditional correlation of expression for g_i and TF_j). The appropriate manner in which to combine direct and indirect evidence remains an open question. Though both measures are bounded by [0,1] their interpretation is quite different. The direct evidence can be considered in terms of it’s conditional gene expression R^2 between nodes, while the indirect evidence is interpreted as a probability. We use a non-parametric approach to combine evidence. The targets of each TF are then ranked and combined as a weighted sum, $w_i = (1 - \alpha) [rank(d_i)] + \alpha [rank(e_i)], i \in \{1, \dots, n\}$. Our choice of the weight, α , here is based on empirical evaluation, and perhaps not surprisingly, is loosely correlated with organism complexity. In validation sets from Yeast, the optimal alpha was observed near $\alpha = .9$ while simpler *E. coli* datasets saw an optimal value of $\alpha = .6$ and an in silico dataset, optimal α was achieved at $\alpha < .5$. This naturally reflects the fact that the increased complexity of the network necessitates the use of larger scale agreement between genes, rather than a reliance on pairwise correlations between potentially noisier and more complex expression patterns.

Network edges are recovered in In Silico, *E. coli* and Yeast(*Saccharomyces cerevisiae*). A common challenge in gene regulatory network inference is the difficulty of validating identified networks against a known, reliable gold standard. A number of validation methods have been used for in vivo samples, including ChIP-seq, ChIP-chip. Knockdowns have also been used in cell lines and have been shown to be effective at predicting in vivo responses [39]. Additionally, in silico methods have been used which simulate gene expression datasets based on a predefined set of regulatory mechanisms.

To test our methods, we used four test datasets of increasing biological complexity- (1) in silico, (2) *E. coli*, and (3) Yeast with simulated motif priors and (4) Yeast with biological motif priors. Data from (4) was collected from *Saccharomyces cerevisiae* with TF knock-out and stress conditions [42]. Data from the first three sources was obtained from the publicly available DREAM5 challenge[43]. This challenge asked contestants to infer gene networks from expression data alone, using a gold standard for evaluation. Instead, we started with the gold standard and swapped a number of edges to create the type I and type II error rates consistent with Yeast motif priors and evaluated the performance of MONSTER to refine its predictions of the true gold standard. The estimated edges in MONSTER utilizing the gene expression data were demonstrated to be superior to those of the edge prior alone.

Computation of MONSTER’s transition matrix. A primary purpose of reconstructing GRNs is the understanding of the biological mechanisms which characterize disease. Identifying differential TF targeting may suggest a therapeutic target, uncover a disease substructure or identify biomarkers for early detection. However, significant limitations exist with respect to generating reliable context-specific GRNs. Substantial advances have

been made in this area with algorithms like SEREND and PANDA, but these methods rely more heavily on the static sequence motif data rather than gene expression data collected across groups, such as in a case-control study. Both methods, along with MONSTER’s network inference approach, use gene expression data as a refinement of the more accurate motif priors. It is therefore a side effect that any GRN inference method that relies on motifs directly for edge-weight calculation will be susceptible to having the bulk of its predictive power stripped when making comparisons between networks. Consequently, it is of critical importance to choose a network inference method that uses the context-specific data to most accurately refine above what information is gleaned from our static data.

The task of identifying meaningful network transitions then becomes an evaluation of the relative refinement of edge-weights. Since the majority of the predictive power for each edge is contained in the motif contribution, we are left with relative edge-weight refinement that have a low signal, high noise. In other words, we have a very large number of individually unreliable edge-weights. In effort to extract the maximum effect, we seek to combine the information contained in each edge via a novel dimension reduction approach.

Consider two adjacency matrices, \mathbf{A}, \mathbf{B} representing the two GRNs estimated from a case-control study. Each matrix has dimensions $(p \times m)$ representing the set of p genes targeted by m TFs. We seek a matrix, \mathbf{T} , such that

$$\mathbf{B} = \mathbf{AT} + \mathbf{E}$$

Where \mathbf{E} is our error matrix, which we want to minimize. Intuitively, we may frame this as a set of m independent regression problems, where m is the number of transcription factors and also the column rank of $\mathbf{A}, \mathbf{B}, \mathbf{T}$ and \mathbf{E} . For a column in \mathbf{B} , \mathbf{b}_i , we note that a corresponding column in \mathbf{T} , τ_i , represents the OLS solution to

$$E[\mathbf{b}_i] = \tau_{i1}\mathbf{a}_{1i} + \tau_{i2}\mathbf{a}_{2i} + \dots + \tau_{im}\mathbf{a}_{mi}$$

or alternatively expressed

$$\begin{bmatrix} \mathbf{b}_{i1} \\ \mathbf{b}_{i2} \\ \vdots \\ \mathbf{b}_{ip} \end{bmatrix} = \tau_{1,i} \begin{bmatrix} \mathbf{a}_{11} \\ \mathbf{a}_{21} \\ \vdots \\ \mathbf{a}_{p1} \end{bmatrix} + \dots + \tau_{p,i} \begin{bmatrix} \mathbf{a}_{1p} \\ \mathbf{a}_{2p} \\ \vdots \\ \mathbf{a}_{pp} \end{bmatrix} + \begin{bmatrix} e_{i1} \\ e_{i2} \\ \vdots \\ e_{ip} \end{bmatrix}$$

$$\text{where } E[e_{ij}] = 0$$

This can be solved with normal equations,

$$\begin{aligned} \tau_i &= (\mathbf{A}^T \mathbf{A})^{-1} \mathbf{A}^T \mathbf{b}_i \\ \mathbf{T} &= [\tau_1, \tau_2, \dots, \tau_m] \end{aligned}$$

Which produces the least squares estimate. I.e. loss function $L(\mathbf{T}) = \sum_{gene=1}^N ||\mathbf{B}_{gene} - \mathbf{A}_{gene} \mathbf{T}||^2$ is minimized. It is easy to see how this approach allows for a straightforward extension via the inclusion of a penalty term. An L_1 regularization[44] may be used by creating an identity penalty model matrix for each column regression such that only the k^{th} diagonal element is 0 and all other diagonals are 1. This gives priority for the k^{th} regression coefficient in the k^{th} regression model.

$$\mathbf{Q}_{i,j} = \begin{cases} 1 & \text{for } i = j \neq k \\ 0 & \text{elsewhere} \end{cases}$$

which results in the minimization of the penalized squared loss function

$$\sum_{i=1}^p \left(\mathbf{B}_{i,k} - \sum_{j=1}^m A_{i,j} \mathbf{T}_{j,k} \right)^2 + \lambda \sqrt{\beta' \mathbf{Q} \beta}$$

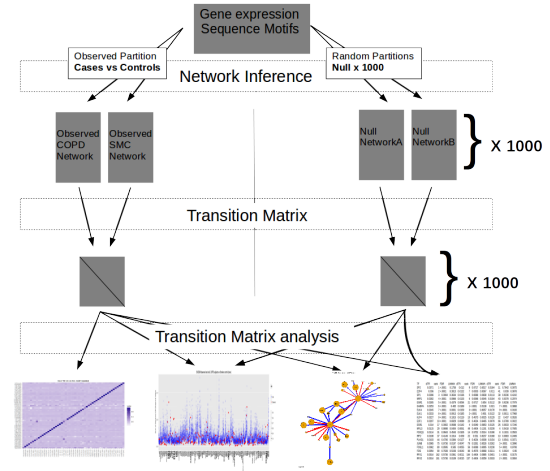
This illustrates a key feature of this method. Specifically, that the transition matrix reduces the case-control network transformation from a set of $2 \times p \times m$ estimates to a set of $m \times m$ estimates that are easily interpreted. We can think of a column, τ_i , on the matrix \mathbf{T} as containing the linear combination of regulatory targets of TF_i in \mathbf{A} that best approximates the regulatory targets of TF_i in \mathbf{B} . As one would expect, a large proportion of the matrix "mass" would be on the diagonal for those TFs which do not change regulatory behavior between case and control. It is therefore of interest to evaluate values off of the diagonal as indications of a network transition.

Evaluating the Transition Matrix. Many mechanisms which may be differentially present, such as RNA degradation, post-translational modification, protein-level interactions and epigenetic alterations have the ability to impact downstream targeting without impacting the expression level of the TF itself. It may be of particular scientific or therapeutic interest to identify those TFs which have undergone significant overall changes in behavior between controls and cases. With that objective in mind, we express the statistic- differential Transcription Factor Involvement (DTFI), as a measure for quantifying this property.

$$s_j = \frac{\sum_{i=1}^m I(i \neq j) \tau_{i,j}^2}{\sum_{i=1}^m \tau_{i,j}^2}$$

DTFI can be loosely interpreted as the proportion of TF targeting patterns which is explained by the targeting patterns of other available TFs. This measure, a statistic on the interval $[0, 1]$ seeks to elucidate transitions which are systematic, informative, and non-arbitrary in nature by capturing only the edge-weight signal for which there is an attributable regulatory pattern. The distribution of this statistic under the null has a mean and standard deviation which depend on the motif structure. In particular, both mean and standard deviation are increased for TFs which have fewer prior regulatory targets. From a statistical perspective, TFs with relatively more targets are able to generate more stable targeted expression patterns, which leads to more consistent estimates in "agreement" algorithms such as PANDA. From a biological perspective, increased motif presence may indicate that the TFs are more likely to be ubiquitous housekeeping proteins that do not meaningfully alter their involvement between cases and controls. The dependence of the null distribution on the motif structure is addressed via the following resampling procedure.

1. Gene expression samples are randomly assigned to case and control forming the null-case and null-control with group sizes preserved.
2. GRNs are reconstructed for the null-case and null-control with the same prior regulatory structure.
3. The transition matrix algorithm is applied for the two null networks.
4. The differential TFI is calculated for each TF.



Supporting Figure 3. Overview of MONSTER analysis workflow. (1) Network inference is computed separately to subsets of the gene expression data including the cases group, the controls group and 1000 permutations of the cases and controls labels. (2) Transition matrix is estimated between the cases and controls and each of the pair or permuted "cases" and "controls".

5. Repeat 1-4 1000 times.

MONSTER significantly improves TF-TF edge estimation from *in silico* gene expression data. To evaluate the ability of our method to recover edges between transcription factors, we generated simulated gene expression data. We began by randomly generating a true controls adjacency matrix, $M_0(p \times m)$, describing the weighted edges between $m = 100$ transcription factors and $p = 10000$ genes. We initially set a cases network, $M_1(p \times m)$, equal to the controls network- representing no state transition. A state transition was then generated by sampling 100 TF-TF pairs and adjusting the edge-weight at the corresponding point on the true cases adjacency matrix. These TF-TF pairs ultimately represent the edges that we seek to recover and the size of the adjustments are the parameters of interest.

We sampled from a multivariate Gaussian distribution with the off-diagonal of the variance-covariance matrix, Σ , defined as $M_0 M_0'$ and $M_1 M_1'$ for controls and cases, respectively. Furthermore, we scaled the magnitude of the diagonal of Σ to achieve the desired proportion of noise. We aimed for an area under the curve of the receiver-operator characteristic of approximately 0.70 as this has been achieved in existing network inference studies [8].

This sampling generated our simulated 100 case and 100 control samples. Next, we reconstructed the networks from our expression data using a set of commonly used network inference methods - Weighted Gene Correlation Network Analysis (WGCNA) [45] [46], Topological Overlap Measure (TOM) [47], Algorithm for the Reconstruction of Gene Regulatory Networks (ARACNE) [16], Context Likelihood of Relatedness (CLR) [17], and simple Pearson correlation (PC). Each method was implemented using the R package nettools [?].

This yield a case and control network for each of the six methods being tested. As a benchmark we measured the area-under-the-curve of the receiver-operator-characteristic (AUROC) for each method using the top 100,000 true edgeweights as a gold standard.

AUC-ROC for edge-weight differences vs Transition Matrix using various NI methods

NI Method	Network AUC	edge-weight differences	MONSTER
Pearson	.704	.510 ($p=.72$)	.802 ($p<.0001$)
WGCNA(6)	.704	.512 ($p=.61$)	.688 ($p<.0001$)
WGCNA(12)	.704	.52 ($p=.10$)	.589 ($p=.02$)
ARACNE	.515	.523 ($p=.58$)	.566 ($p=.09$)
CLR	.694	.57 ($p=.19$)	.814 ($p<.0001$)
TOM	.703	.51 ($p=.62$)	.689 ($p<.0001$)

Supporting Table 1. Comparison of edge-weight difference to Transition Matrix in simulated case-control gene expression. Several network inference methods were run on our *in silico* case-control data. The overall network area under the curve of the receiver-operator characteristic (AUC-ROC) was performed for each method averaged across cases and controls. The naive TF-TF transitions were calculated as the difference in TF-TF edge-weight between cases and controls. The transition matrix TF-TF transitions used the absolute transition matrix values.

Next, we compared two approaches for identifying TF-TF interactions. (1) Applying the transition matrix with default parameters on each case-control pair of networks and (2) the difference from case to control in edge-weights derived from the direct edge prediction using each network inference method.

The predictions for the TM approach and the direct edge-weight difference approach were evaluated by AUCROC with the true transition adjustments taken as the gold standard. For each of the network inference methods tested, we found substantial improvement in the predicted transitions over the direct edge-weight difference method. In many cases, the edge-weight difference (column 3) was not statistically significant for predicting transitions, but when the TM was applied (column 4) a strong predictive signal appeared. In other cases, an existing signal was observed using the direct approach, but was dramatically improved with the application of the TM.

The intuition behind the improvement is simple. While the estimation of a TF-TF edge is typically evaluated via some pairwise gene expression pattern which may be rife with technical and biological noise, the TM approach borrows information from all downstream targets in estimating the relative change in relationship between the TFs.

MONSTER finds significant protein-protein interaction. As noted above, there are numerous biological regulatory mechanisms which may yield detectable transitions. Of particular interest are those which are less readily detectable via conventional methods, such as differential gene expression analysis. One mechanism studied here involves one TF binding to another TF to promote, suppress or alter one or both of their regulatory patterns. These multi-protein interactions create combinatorial complexity that can explain much of the variation in organism complexity which is unexplained by gene expression alone [48].

To test the ability to detect protein level interactions, we compared our estimated transitions to a set of known protein-protein interactions [49]. This set contained 223 interactions between our set of transcription factors, of which 39 were self-interacting and were removed. We attempted to predict the remaining 184 interactions between transcription factors using

MONSTER. Of interest was the effectiveness of identifying these interactions via the transition from one phenotypic state to another. This is a challenging task for several reasons, (1) protein-protein interaction is merely one of a myriad of detectable transition mechanisms which MONSTER is designed to detect, (2) it is reasonable to assume that only a small subset of the known PPI are actually differentially present between cases and controls in a particular study and (3) technological limitations in the active field of proteomics cannot be expected to identify all interactions with a reasonable degree of certainty.

We measured the ability to identify suspected interactions by running MONSTER on the 84 smoker controls and the 136 COPD patients in the ECLIPSE study. We used the absolute value of each element in the transition matrix to serve as the predictor of PPI and computed the area under the ROC curve. To identify the significance of AUC-ROC, we ran MONSTER on 400 iterations of randomized phenotypic labels and computed the AUC-ROC for each iteration.

We achieved only an AUC-ROC score of .548 suggesting weak predictive power of MONSTER for identifying known PPI in the ECLIPSE study, but this result exceeded all randomized phenotype results and was significant at $p < .0025$. This indicates that this weak, but significant result was driven by the differentiation of COPD patients and smoker controls. Notably, MONSTER was able to extract a small but significant protein interaction signal from highly obfuscated data.

Efficiency of estimation. We demonstrate that MONSTER is more efficient at estimating state transitions than directly comparing the results of coexpression networks under the following assumptions.

Let \mathbf{x}_p be a Gaussian p -vector representing a sample of gene expression data containing m transcription factors and $p - m$ non-transcription factor genes.

$$\mathbf{x}_p \sim N(\mu, \Sigma)$$

where μ is the p -vector of mean gene expression values and Σ is the $p \times p$ variance-covariance matrix. In this scenario, Σ may be regarded as a combination of two independent variance-covariance sources- (1) biological signal, (2) biological noise and technical noise.

In investigating gene regulation, many network inference methods are constructed for the estimation of the $p \times m$ subset of Σ pertaining to the effect of the m TFs on the $p - m$ genes. In identifying drivers of state transitions, we seek to focus on the $m \times m$ matrix of TF-TF effects. We show that our method vastly outperforms commonly used network inference methods in estimating these specific effects.

Consider a state change between two experimental conditions, A and B, characterized by an alteration of size δ to the biological signal component of the TF-TF variance-covariance matrix at point $\Sigma_{i,j}$ where i and j are indices for two TFs in Σ .

Using the difference between the two coexpression calculations (the basis for Pearson networks and WGCNA estimates), the estimated variance of our estimate of δ can be calculated for $-\rho_A < \delta < \rho_A, \delta + \rho_A \leq 1$:

$$-\rho_A < \delta < \rho_A, \delta + \rho_A \leq 1$$

$$\begin{aligned} Var(\hat{\delta}_{cor}) &= Var(\hat{\rho}_{i,j,A} - \hat{\rho}_{i,j,B}) \\ &= Var(\hat{\rho}_{i,j,A}) + Var(\hat{\rho}_{i,j,B}) \\ &= \frac{1 - \rho_{i,j,A}^2}{n_A - 2} + \frac{1 - \rho_{i,j,B}^2}{n_B - 2} \\ &= \frac{1}{n_A - 2} + \frac{1}{n_B - 2} - \frac{\rho_{i,j,A}^2}{n_A - 2} - \frac{\rho_{i,j,B}^2}{n_B - 2} \end{aligned}$$

Meanwhile, in condition B the new correlation of TF_i with some gene, $gene_k$ $k \in 1, 2 \dots p$, denoted cor^* , becomes

$$cor^*(TF_i, gene_k) = cor(TF_i, gene_k) + \delta cor(TF_j, gene_k)$$

where the term $\delta cor(TF_j, gene_k)$ is the change due to the interaction of TF_i and TF_j .

The variance of our estimate using the transition matrix can be expressed as follows:

$$\begin{aligned} Var(TM_{i,j}) &= Var(\hat{\delta}_{TM}) \\ &= \frac{\left(\frac{1}{p}\right) \sum_{k=1}^p vVar(\hat{\rho}_{i,k,A} - \hat{\rho}_{i,k,B})}{\sum_{k=1}^p (\rho_{j,k} - \bar{\rho}_j)^2} \\ &= \frac{\left(\frac{1}{p}\right) \sum_{k=1}^p [Var(\hat{\rho}_{i,k,A}) + Var(\hat{\rho}_{i,k,B})]}{\sum_{k=1}^p (\rho_{j,k} - \bar{\rho}_i)^2} \\ &\leq \frac{\left(\frac{1}{p}\right) \sum_{k=1}^p \left[\frac{1}{n_A-2} + \frac{1}{n_B-2}\right]}{\sum_{k=1}^p (\rho_{j,k} - \bar{\rho}_i)^2} \\ &\leq \frac{\frac{1}{n_A-2} + \frac{1}{n_B-2}}{\sum_{k=1}^p (\rho_{j,k} - \bar{\rho}_i)^2} \\ &\leq \frac{Var(\hat{\delta}_{cor}) + \frac{\rho_{i,j,A}^2}{n_A-2} + \frac{\rho_{i,j,B}^2}{n_B-2}}{\sum_{k=1}^p (\rho_{j,k} - \bar{\rho}_i)^2} \\ &\leq Var(\hat{\delta}_{cor}) + \frac{Var(\hat{\delta}_{cor}) (1 - \sum_{k=1}^p (\rho_{j,k} - \bar{\rho}_i)^2) + \frac{\rho_{i,j,A}^2}{n_A-2} + \frac{\rho_{i,j,B}^2}{n_B-2}}{\sum_{k=1}^p (\rho_{j,k} - \bar{\rho}_i)^2} \end{aligned}$$

So we have that $Var(TM_{i,j}) < Var(\hat{\delta}_{cor})$ when

$$Var(\hat{\delta}_{cor}) \left(1 - \sum_{k=1}^p (\rho_{j,k} - \bar{\rho}_i)^2\right) < \frac{\rho_{i,j,A}^2}{n_A-2} + \frac{\rho_{i,j,B}^2}{n_B-2}$$

Since each term except $(1 - \sum_{k=1}^p (\rho_{j,k} - \bar{\rho}_i)^2)$ is strictly non-negative, we see that this inequality holds when

$$\sum_{k=1}^p (\rho_{j,k} - \bar{\rho}_i)^2 < 1$$

Thus, we have a more efficient estimator of δ when

$$p > \frac{1}{Var(\rho_{j,k})}$$

In practice, we typically have a large number of genes, p , so that our transition matrix estimator will be expected to be dramatically more efficient than the commonly used Pearson or WGCNA estimators for estimating transcription factor-transcription factor interactions.

1. Hill SM et al. (2012) Bayesian inference of signaling network topology in a cancer cell line. *Bioinformatics* 28(21):2804–2810.
2. Glass K et al. (2014) Sexually-dimorphic targeting of functionally-related genes in copd. *BMC systems biology* 8(1):118.

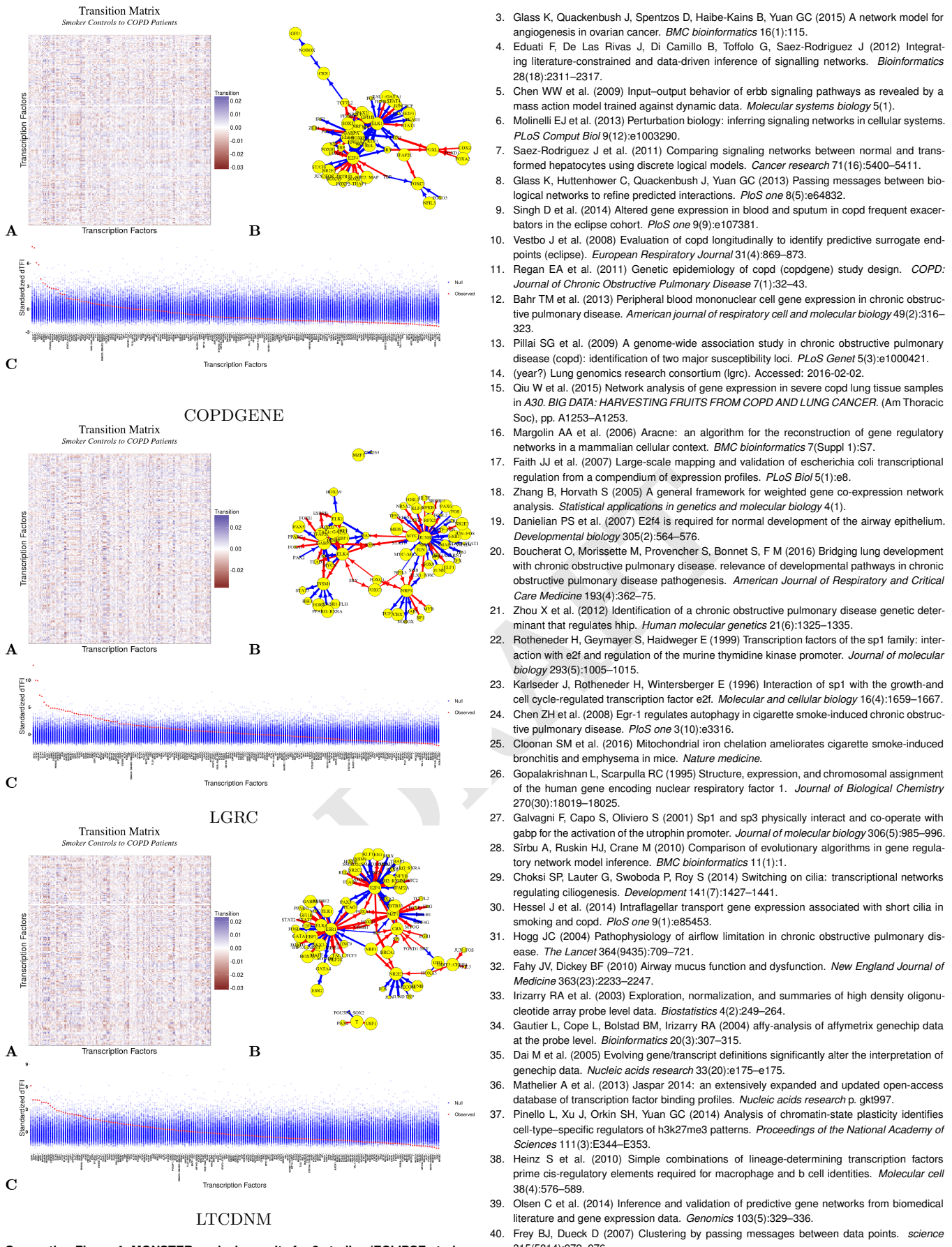
A Top significantly differentially involved transcription factors

TF	ECLIPSE			COPDGene			LGRC			LTCDNM		
	dTFI	rank	FDR	dTFI	rank	FDR	dTFI	rank	FDR	dTFI	rank	FDR
SP2	.0314	1	.0357	.0100	9	.6812	.0213	6	.3752	.0176	2	.7438
E2F4	.0236	2	<.0001	.0143	3	<.0001	.0160	14	.037	.0148	7	<.0001
SP1	.0230	3	.1551	.0089	18	.7721	.0179	10	.3594	.0169	4	.5516
ZNF263	.0226	4	.311	.0089	16	.3372	.0177	11	.7716	.0152	6	.927
EGR1	.0224	5	.1242	.0079	23	.7597	.0124	28	.6892	.0152	5	.5305
NRF1	.0196	6	<.0001	.0115	5	.0304	.0122	30	<.0001	.0139	11	.0558
GABPA	.0185	7	<.0001	.0157	2	<.0001	.0176	12	<.0001	.0097	32	.0853
ELK1	.0177	8	<.0001	.0174	1	<.0001	.0151	17	<.0001	.0083	40	.2099
ZFX	.0175	9	<.0001	.0076	24	.8366	.0103	40	.4348	.0132	16	.2739
KLF4	.0173	10	.1025	.0072	28	.8142	.0143	21	.2312	.0119	20	.5516
ESR1	.0169	11	.0357	.0106	7	.0941	.0127	27	.0888	.0176	3	<.0001
ELK4	.0168	12	<.0001	.0125	4	<.0001	.0152	16	<.0001	.0086	39	.1318
TFAP2C	.0139	17	.0656	.0114	6	.0941	.0148	19	.037	.0121	19	.2099
PLAG1	.0124	21	.263	.0092	15	.4136	.0219	5	<.0001	.0146	8	.1554
FOXQ1	.0115	28	.9318	.0099	10	.7905	.0209	7	.2846	.0107	27	.927
FOSL1	.0082	57	.9175	.0061	41	.6166	.0220	4	.037	.0131	17	.3496
NFIL3	.0077	62	.2365	.0067	33	.0304	.0264	1	.4669	.0209	1	.7121
FOS	.0068	73	.9175	.0057	48	.5212	.0198	9	.037	.0112	24	.5139
JUNB	.0067	77	.9318	.0059	43	.6392	.0236	2	<.0001	.0146	9	.2299
RFX1	.0019	159	.3532	.0009	164	<.0001	.0233	3	<.0001	.0070	48	.3496
RFX2	.0019	158	.4041	.0012	163	.0482	.0200	8	<.0001	.0049	81	.6245

B Differential gene expression for significantly involved transcription factors.

TF	ECLIPSE		COPDGene		LGRC		LTCDNM	
	dTFI rank	LIMMA p						
SP2	1	.1756	9	.6517	6	.0075	2	.0009
E2F4	2	.3913	3	.9367	14	.0878	7	.8232
SP1	3	.3634	18	.0838	10	.4242	4	.9759
ZNF263	4	.9834	16	.0028	11	.0271	6	.1859
EGR1	5	.4379	23	.8540	28	.7979	5	.0378
NRF1	6	.0966	5	.0045	30	.2974	11	.3418
GABPA	7	.4650	2	.5138	12	.3868	32	.5771
ELK1	8	.0913	1	.9010	17	.7968	40	.0005
ZFX	9	.8253	24	.5795	40	.0474	16	.1572
KLF4	10	.1915	28	.0025	21	.0526	20	.1159
ESR1	11	.9598	7	.5853	27	.7246	3	.3477
ELK4	12	.0001	4	.8057	16	.0183	39	.7314
TFAP2C	17	.2318	6	.9574	19	.5853	19	.6754
PLAG1	21	.0384	15	.0008	5	.0371	8	.9523
FOXQ1	28	.4543	10	.5314	7	.0503	27	.5340
FOSL1	57	.5850	41	.6995	4	.8708	17	.3686
NFIL3	62	.0404	33	.1191	1	.7605	1	.8650
FOS	73	.5156	48	.6668	9	.9500	24	.7891
JUNB	77	.0197	43	.9526	2	.3996	9	.6077
RFX1	159	.0361	164	.0885	3	.0175	48	.8285
RFX2	158	.0109	163	.0059	8	.0004	81	.1345

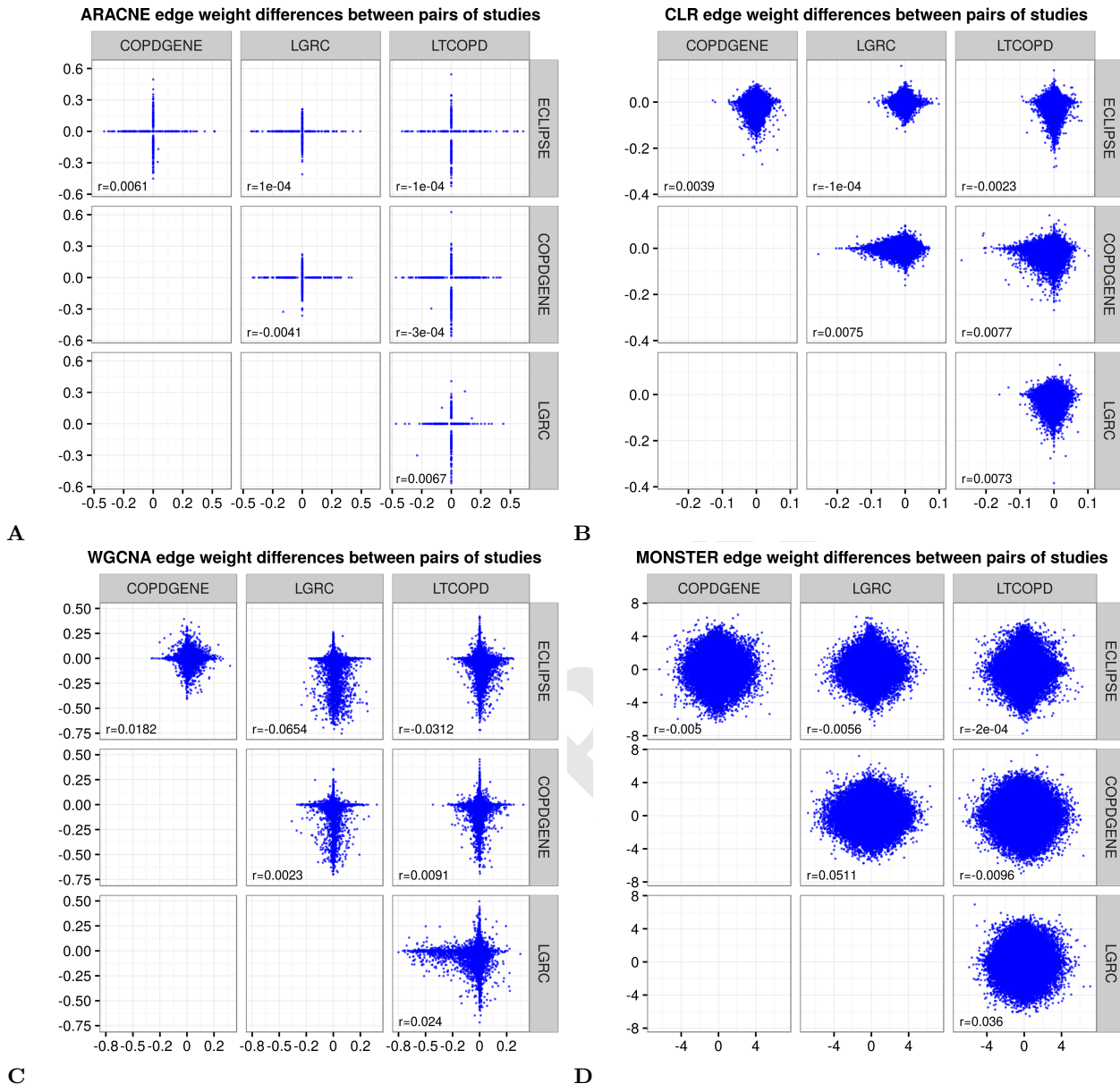
Supporting Table 2. Top Transcription Factor Hits. A Combined list of TFs which were among the top 10 hits (out of 166 available TFs) in any of the 4 studies, ordered by the dTFI in the ECLIPSE study. For each study, columns indicate the TF's (1) differential TF Involvement, (2) dTFI Rank within list of TFs, (3) and Significance of dTFI by false discovery rate. B The same list of top transcription factors evaluated for differential gene expression with p-value for differential gene expression analysis using LIMMA [50]. Notably, a substantial number of differentially involved transcription factors do not exhibit gene expression differentiation, highlighting the ability of MONSTER to identify key features distinguishing phenotypes which are not detectable via gene expression analysis.



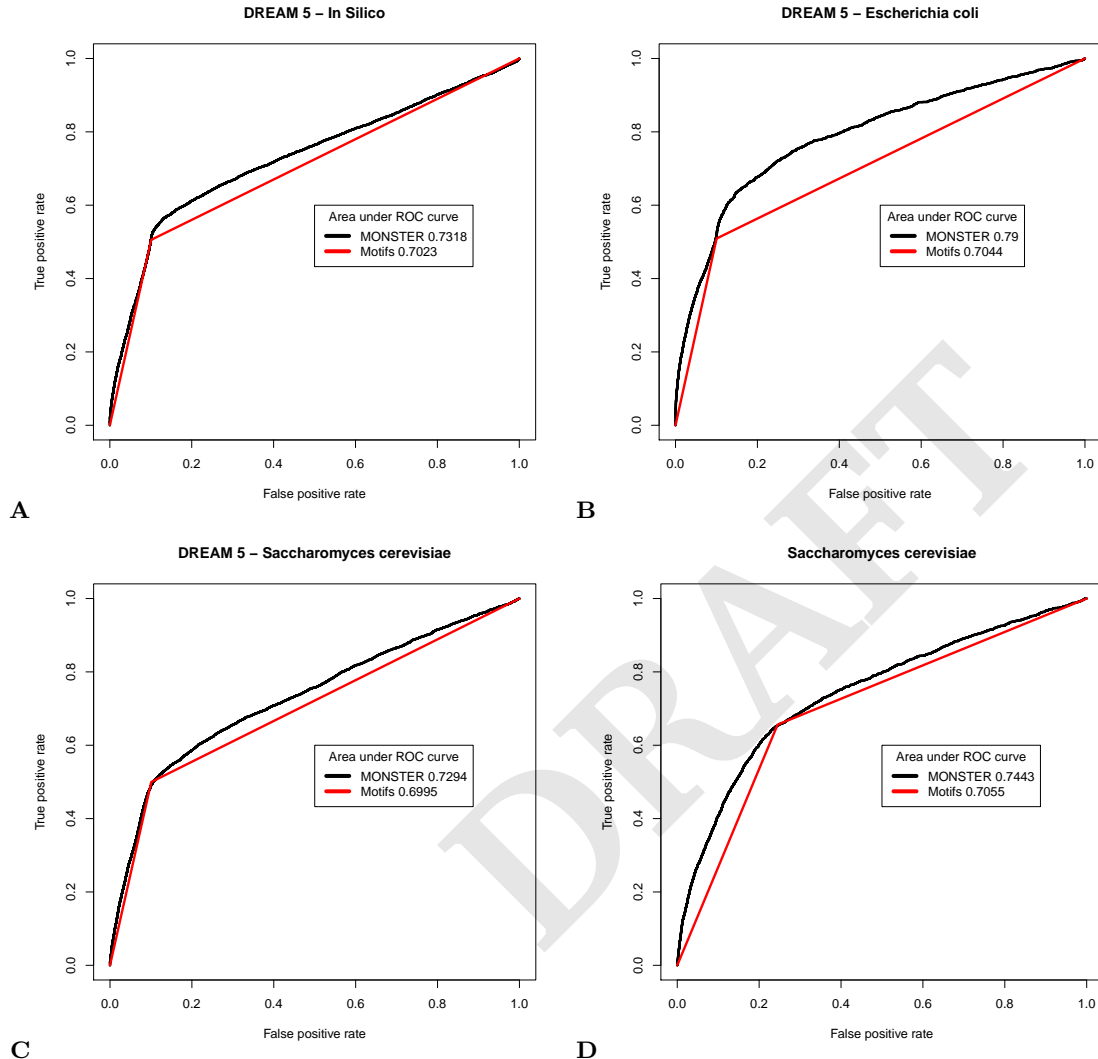
Supporting Figure 4. MONSTER analysis results for 3 studies (ECLIPSE study is found in Fig. 2) A Heatmap depicting the transition matrix calculated from smoker controls to COPD cases by applying MONSTER to three independent COPD studies. Schrödinger's principle of visualization, the magnitude of the diagonal is set to zero. B A network visualization of the strongest 100 transitions identified based on the transition matrix shown in A. Arrows indicate a change in edges from a transcription factor in the Smoker-Control network to resemble those of a transcription factor in the COPD network. Edges are sized according to the magnitude of the transition and nodes

41. Lao T et al. (2015) Haploinsufficiency of hedgehog interacting protein causes increased emphysema induced by cigarette smoke through network rewiring. *Genome medicine* 7(1):1.
42. Harbison CT et al. (2004) Transcriptional regulatory code of a eukaryotic genome. *Nature* 431(7004):99–104.
43. Marbach D et al. (2012) Wisdom of crowds for robust gene network inference. *Nature methods* 9(8):796–804.
44. Tibshirani R (1996) Regression shrinkage and selection via the lasso. *Journal of the Royal Statistical Society. Series B (Methodological)* pp. 267–288.
45. Langfelder P, Horvath S (2008) Wgcna: an r package for weighted correlation network analysis. *BMC Bioinformatics* (1):559.
46. Langfelder P, Horvath S (2012) Fast R functions for robust correlations and hierarchical clustering. *Journal of Statistical Software* 46(11):1–17.
47. Ravasz E, Somera AL, Mongru DA, Oltvai ZN, Barabási AL (2002) Hierarchical organization of modularity in metabolic networks. *science* 297(5586):1551–1555.
48. Levine M, Tjian R (2003) Transcription regulation and animal diversity. *Nature* 424(6945):147–151.
49. Ravasi T et al. (2010) An atlas of combinatorial transcriptional regulation in mouse and man. *Cell* 140(5):744–752.
50. Ritchie ME et al. (2015) limma powers differential expression analyses for rna-sequencing and microarray studies. *Nucleic acids research* p. gkv007.

DRAFT

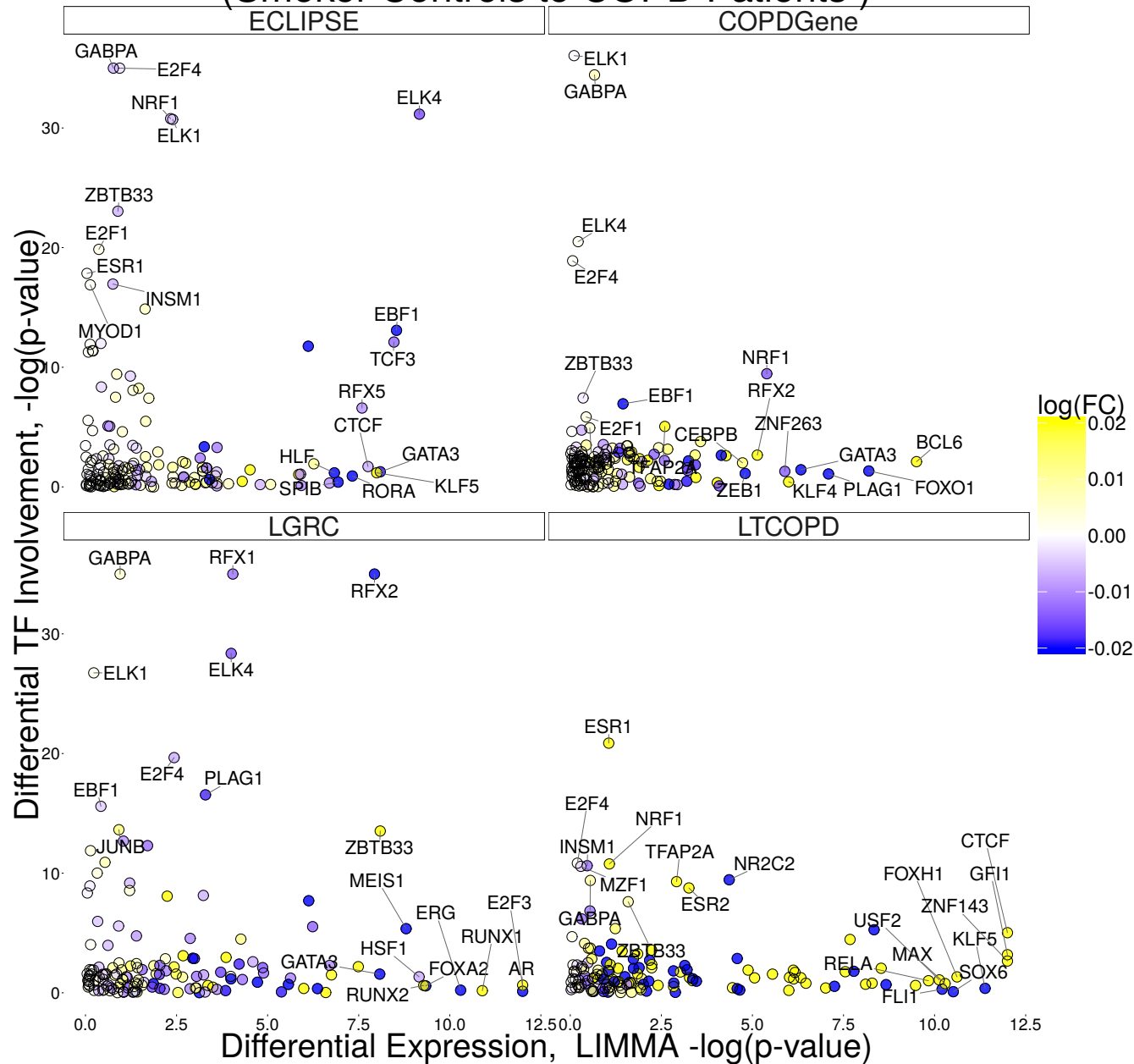


Supporting Figure 1. edge-weight differences between cases and controls do not correlate across studies. Using three commonly used network inference methods from gene expression data, network inference was performed separately on cases and controls. Here, the case-control difference is compared across four independent studies of COPD. The methods tested were **A** Algorithm for the Reconstruction of Gene Regulatory Networks (ARACNE), **B** Context Likelihood of Relatedness (CLR), **C** Weighted Gene Correlation Network Analysis (WGCNA), and **D** MONSTER. No detectable agreement between studies exist were found, regardless of network inference method or tissue type.



Supporting Figure 2. Receiver-Operator Characteristic curves for three DREAM 5 datasets (A) in silico, (B) E. coli, (C) *Saccharomyces cerevisiae*, and an (D) independent *Saccharomyces cerevisiae* dataset. The initial prior network in each of the DREAM 5 datasets was taken from the gold standard, with error introduced (both type I and type II) bringing the area under the ROC curve to ≈ 0.70 . In the *Saccharomyces cerevisiae*, sequence motifs were used as the prior with ChIP-chip binding sites used as the gold standard. In each of these tests, measurable improvement in performance of MONSTER's network inference method over the prior network is observed.

Differential Involvement vs Differential Expression (Smoker Controls to COPD Patients)



Supporting Figure 5. Differentially transcription factor involvement vs differential gene expression in four studies of COPD. MONSTER commonly finds transcription factors which are differentially involved but are expressed at similar levels across cases and controls. Likewise, differential expression does not indicate differential involvement in MONSTER. For those transcription factors which are differentially involved, but not differentially expressed, the change in involvement suggests behavioral alterations at a post-transcriptional stage. Importantly, the results found in this scenario could not have been identified using conventional differential expression methods.